

Losses Analysis of Induction Motors under Ambient and Cryogenic Conditions

*Original*

Losses Analysis of Induction Motors under Ambient and Cryogenic Conditions / Bucho, L.F.D., Fernandes, J.F.P., Costa Branco, P.J., BIASION, M., Vaschetto, S., Cavagnino, A.. - ELETTRONICO. - (2022), pp. 01-07. (2022 IEEE Energy Conversion Congress and Exposition (ECCE) Detroit, MI, USA Ottobre 2022) [10.1109/ECCE50734.2022.9947595].

*Availability:*

This version is available at: 11583/2982559 since: 2023-09-28T16:15:54Z

*Publisher:*

IEEE

*Published*

DOI:10.1109/ECCE50734.2022.9947595

*Terms of use:*

This article is made available under terms and conditions as specified in the corresponding bibliographic description in the repository

*Publisher copyright*

IEEE postprint/Author's Accepted Manuscript

©2022 IEEE. Personal use of this material is permitted. Permission from IEEE must be obtained for all other uses, in any current or future media, including reprinting/republishing this material for advertising or promotional purposes, creating new collecting works, for resale or lists, or reuse of any copyrighted component of this work in other works.

(Article begins on next page)

# Losses Analysis of Induction Motors under Ambient and Cryogenic Conditions

Luis F. D. Bucho  
IDMEC, Instituto Superior Técnico,  
University of Lisbon,  
Lisbon, Portugal  
luis.bucho@tecnico.ulisboa.pt

João F. P. Fernandes, *Member, IEEE*  
IDMEC, Instituto Superior Técnico,  
University of Lisbon,  
Lisbon, Portugal  
joao.f.p.fernandes@tecnico.ulisboa.pt

P. J. Costa Branco, *Member, IEEE*  
IDMEC, Instituto Superior Técnico,  
University of Lisbon,  
Lisbon, Portugal  
pbranco@tecnico.ulisboa.pt

Marco Biasion, *Student Member, IEEE*  
Dipartimento Energia  
Politecnico di Torino  
Torino, Italy  
marco.biasion@polito.it

Silvio Vaschetto, *Senior Member, IEEE*  
Dipartimento Energia  
Politecnico di Torino  
Torino, Italy  
silvio.vaschetto@polito.it

Andrea Cavagnino, *Fellow, IEEE*  
Dipartimento Energia  
Politecnico di Torino  
Torino, Italy  
andrea.cavagnino@polito.it

**Abstract**—Cryogenic induction machines have been re-emerging as a potential solution to increase the current power density for challenging specific power applications. Compared with an ambient temperature operation, cryogenic conditions allow higher power density and increased efficiency due to the decrease of electric resistivity of conducting materials and increased cooling capability. This work focuses on the losses analysis of induction machines immersed in liquid nitrogen. Under ambient and cryogenic conditions, experimental tests are performed and presented for two induction machines, a 90 W 40 V induction machine, and a 550 W 400 V induction machine, to evaluate the mechanical, iron and residual losses, and the change of their equivalent circuit parameters.

**Keywords**—Cryogenics, electromagnetic measurements, induction motor, loss segregation, performance, temperature impact.

## I. INTRODUCTION

In 2011, the European Union defined goals for reducing CO<sub>2</sub>, NO<sub>x</sub>, and noise emissions by 75%, 90%, and 65% for commercial aircraft by 2050 [1], [2]. These targets led to new higher specific power and efficiency requirements for electrical machines. Cryogenic cooled machines are potential solutions to meet these requirements. In fact, the operation of electric machines in a cryogenic environment allows considerable improvements in specific power and efficiency. Examples are cryogenic induction machines (IM) that have been used in cryogenic pumps operating with liquefied natural gas (~110 K) and missile cryogenic propellant systems using liquid hydrogen (~20 K) [3], [4]. Cryogenic motors for different industrial applications are usually first tested under liquid nitrogen (LN<sub>2</sub>) for safety reasons. Therefore, testing an induction machine under LN<sub>2</sub> is an important research work for its behavior and performance characterization under cryogenic conditions.

The effects of low temperature in induction motors are various. First, it is well known that the resistivity of both copper and aluminum shows a significant decrease when operating at liquid nitrogen temperatures (77 K) [5], [6]. However, the skin effect cannot be neglected, especially for the rotor cage resistance. In fact, with the temperature reduction, the skin effect increases and the decrease of rotor cage resistance may be limited.

Regarding iron losses, despite recent efforts to study this phenomenon, there is a lack of information on magnetic and loss properties of soft-magnetic materials under cryogenic temperatures [7]-[10]. In general, iron losses in magnetic materials show an increase of 10% to 20% at 77 K relative to ambient temperature operation at industrial frequencies of  $f = 50\text{Hz}$  [7], [11], [12]. This increase in total iron losses is mainly due to the increase in eddy current losses due to the increase of conductivity of the ferromagnetic core laminations [9]-[13]. Moreover, while it is usually considered that hysteresis losses remain approximately constant with the decrease of temperature, some considerations must be taken into account. The estimation of the aggregate effect of all these phenomena is not trivial, given the significant dependence of magnetic properties on grain size, manufacturing process, heat treatment, impurities, and saturation level. For example, it has been shown that the maximum magnetic permeability of high-grade soft iron cores increases under cryogenic conditions, due to the reduction of thermal vibration of lattices [9]. However, compressive mechanical stresses on the iron core due to thermal contraction may also cause an opposite decrease in magnetic permeability [14], [15]. On the other hand, a slight increase of the coercive force  $H_c$  is reported [13].

In addition, under wet cryogenic conditions, due to the presence of liquid nitrogen inside the machine, an increase in mechanical losses is expected, specifically due to windage losses. Although analytical models for windage losses do exist, these do not consider the complexity of the stator and rotor geometries [16], [17]. Furthermore, air gap fluid flow regime identification makes it difficult to estimate this increase without using CFD [10], [18]. This study evaluates the change in mechanical loss based on empirical measurements.

Therefore, with these phenomena combined, under wet cryogenic conditions, positive effects on the induction machine performance, such as the reduction of stator and rotor Joule losses, but also negative effects as the typical increase of mechanical and iron losses are expected. The balance between these effects must be analyzed to verify its impact on machine performance. Hence, this work focuses on the losses analysis of conventional induction motors cryocooled by immersion in liquid nitrogen (77 K).

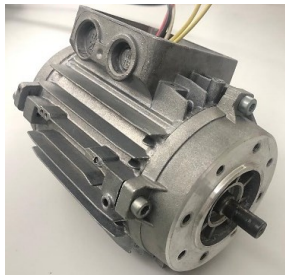


Fig. 1. The 90W TENV induction motor.



Fig. 2. The 550W TENV induction motor.

TABLE I RATED VALUES FOR THE TESTED 90W IM

Parameter	Rated Values
Voltage	40 V
Current	3.6 A
Power	90 W
Speed	1350 rpm
Frequency	50 Hz
cosφ	0.61

TABLE II RATED VALUES FOR THE TESTED 550W IM

Parameter	Rated Values
Voltage	400 V
Current	1.6 A
Power	550 W
Speed	910 rpm
Frequency	50 Hz
cosφ	0.73

In particular, the goal of the research activity is to quantify performance changes from ambient to wet cryogenic conditions, focusing on the variations of the different loss contributions. In this paper, two induction motors are used to experimentally analyze the losses under ambient and cryogenic conditions: a 90 W 40 V IM, and a 550 W 400 V IM. Joule losses in the stator and rotor, mechanical losses and iron losses are investigated at different supply frequencies and compared with their values at ambient temperature operation. This study also presents preliminary considerations on residual losses at cryogenic conditions to complete the analysis.

## II. METHODOLOGY

This study is conducted experimentally with two totally enclosed non-ventilated (TENV) induction machines: *i*) a 90 W, 40 V, 50 Hz, four-pole induction machine previously characterized in [11] and [19] – see Fig. 1, and *ii*) a 550 W, 400 V, 50 Hz, six-pole induction machine – see Fig. 2.

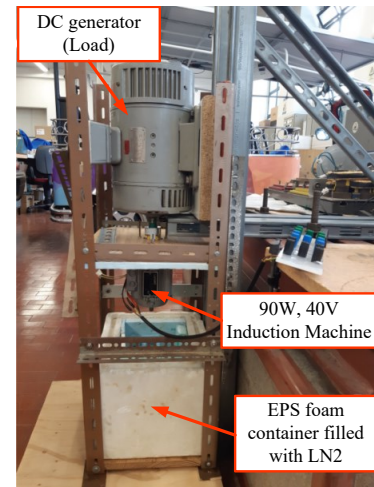


Fig. 3. Experimental setup associated to the 90 W induction machine.

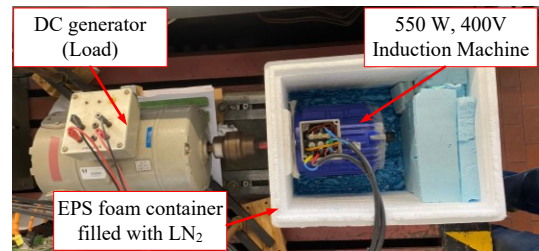


Fig. 4. Experimental setup associated to the 550 W induction machine.

Their rated values are listed in Table I and Table II, respectively. Both IMs have stator copper distributed windings, a FeSi alloy iron core and a rotor cage made of aluminum die-cast. The IMs are tested under ambient and cryogenic conditions using the experimental setups shown in Fig. 3 and Fig. 4. The vertical setup revealed to be stable for testing the 90 W IM, due to its low weight and size. However, a horizontal setup was required for the 550 W IM, to mitigate increased vibrations due to its higher size and weight. An EPS foam container filled with liquid nitrogen is used to cool the two IMs by immersion. In addition, the grease of the bearing was removed because it freezes under cryogenic conditions. This was done using a bath of acetone for 5 days.

No-load, locked rotor, and load tests were performed, for both machines at ambient and cryogenic conditions, following the IEC 60034-2-1 procedure. Although test procedures prescribed by efficiency standards for conventional IMs do not apply to IMs under cryogenic conditions, variable load tests according to IEC 60034-2-1 have also been conducted to discuss the residual losses behavior under these conditions. From the no-load and locked rotor tests, the parameters of the single-phase equivalent circuit can be computed, as well as the mechanical and iron losses.

At no-load tests, the induction machines were supplied by a three-phase sinusoidal stator voltage from 110% of its rated voltage down to 30%. In addition, for the 90 W IM, no-load tests were conducted at different supply frequencies,  $f = [20, 30, 40, 50]$  Hz, to characterize the change of mechanical losses and iron losses with different speeds and electric frequencies.

TABLE III STEADY-STATE EQUIVALENT CIRCUIT PARAMETERS AT 50 HZ FOR THE 90 W IM AT AMBIENT AND CRYOGENIC CONDITIONS

Parameter	Amb.	Cryo.	Difference
$R_s$	1.10 $\Omega$	0.175 $\Omega$	-84.1%
$R'_r$	0.914 $\Omega$	0.240 $\Omega$	-73.4%
$X_{\sigma s}$	0.532 $\Omega$	0.532 $\Omega$	0%
$X'_{\sigma r}$	0.532 $\Omega$	0.532 $\Omega$	0%
$R_{fe}$	116.4 $\Omega$	104.3 $\Omega$	-10.4%
$X_m$	7.33 $\Omega$	7.24 $\Omega$	-1.2%

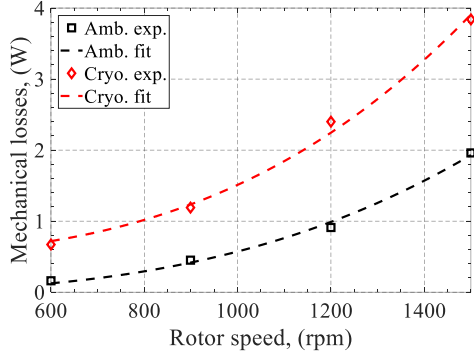


Fig. 5. Mechanical losses as a function of the rotor speed.

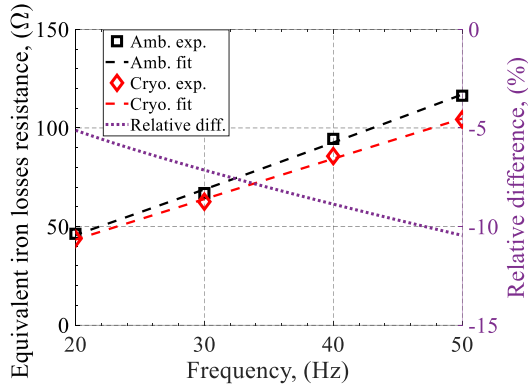


Fig. 6. Iron losses resistance as a function of the frequency.

At frequencies different than 50 Hz, the considered rated voltage was defined using a scalar command to assure the same rated magnetizing flux. For the 550 W IM, no-load tests were conducted at 50 Hz, and in future research activities, these will also be carried out at different electric frequencies.

At ambient temperature conditions, the locked-rotor tests were performed with different stator currents up to the rated value. However, the stator current was increased under cryogenic conditions due to the lack of thermal limitation. For the 90 W IM, the stator current reached around 10 A, and for the 550 W IM, the stator current reached 3.2 A.

Rated and variable load tests were conducted to evaluate the loss separation and the consequent determination of the residual losses.

### III. RESULTS AND DISCUSSION

The experimental results for both IMs, under ambient and cryogenic conditions, are presented and discussed.

#### A. 90 W Induction Motor

The equivalent circuit parameters of the 90 W induction machine, determined experimentally for a frequency of 50 Hz, are summarized in Table III. During the testing activities, the stator windings and rotor temperatures were measured with cryogenic temperature sensors, capable of operating in a wide range of temperatures (from -200 °C up to +600 °C). At ambient conditions, the stator windings and rotor aluminum cage operate at around 40 °C and 60 °C, respectively, while at cryogenic conditions their temperatures are around -196 °C (77 K). As shown in Table III, due to the high temperature decrease, there is a reduction of 84.1% for the stator resistance and 73.4% for the rotor resistance. This effect is related to the reduction of copper and aluminum electric resistivities under cryogenic conditions. In addition, the iron losses increased by 11.6%, leading to a decrease of 10.4% of the iron losses resistance. As shown in previous works, a negligible change in the  $BH$  curve for silicon-iron materials is verified at 77 K and  $f=50$  Hz [11]. Thus, the increase of iron losses is mostly related to the increase of eddy currents.

A minor change of stator, rotor and magnetizing reactances was observed for this machine. This is in line with the results presented in [11], where a negligible influence of the skin effect was found on the stator and rotor leakage and magnetizing reactances.

Figure 5 presents the results of mechanical losses at different rotor speeds. The experimental points were fitted using a cubic function with the frequency. The coefficient of the cubic interpolation increased 77% when in cryogenic conditions. This increase is mainly due to the presence of liquid nitrogen inside the airgap of the machine and inside the bearings. At rated conditions, the mechanical losses increased from 1.96 W at ambient conditions to 3.83 W at cryogenic conditions, leading to a 95.4% increase. The change of equivalent iron losses resistance with different frequencies is presented in Fig. 6. Results show a linear behavior of the iron losses resistance with the frequency at both ambient and cryogenic conditions. This indicates that hysteresis losses are predominant at 50 Hz, which is coherent with the results from [7], [20]. Under cryogenic conditions, the iron losses resistance presents a decrease of around -5% at 20 Hz to around -10% at 50 Hz, when compared with ambient temperature conditions. This decrease should be further investigated for higher electric frequencies and higher power IMs, to analyze the change of hysteresis and eddy current losses and of the skin effect under cryogenic conditions.

The results from the load tests under ambient and cryogenic conditions are presented in Fig. 7a and Fig. 7b, respectively. The active power absorbed by the machine is divided into mechanical losses,  $P_{mec}$ , iron losses,  $P_{fe}$ , stator windings losses,  $P_{cuS}$ , rotor losses,  $P_r$ , and output power,  $P_{out}$ , following the IEC 60034-2-1 procedure. The stator copper losses,  $P_{cuS}$ , are obtained from the stator resistance and stator current values.

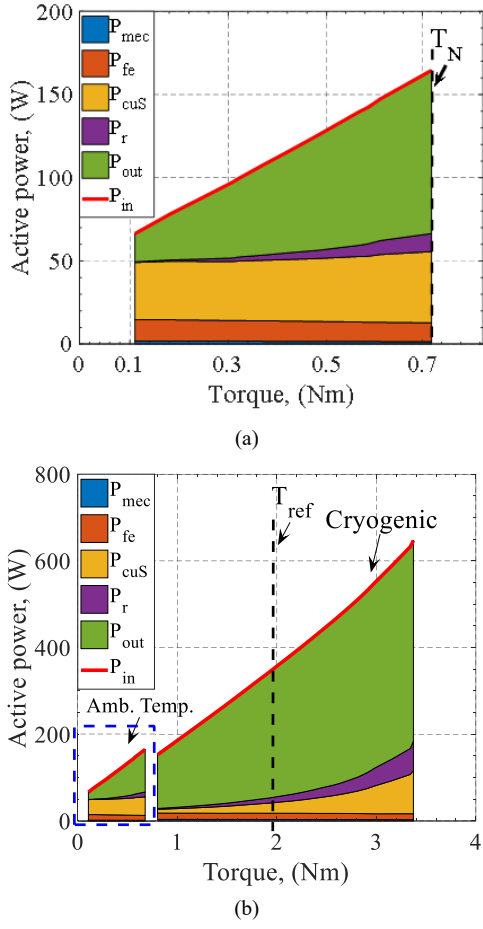


Fig. 7. Separation of active power into losses and output power for the 90 W IM at (a) ambient temperature, and (b) cryogenic conditions.

TABLE IV SUMMARIZED PERFORMANCE FOR THE 90 W IM AT MAXIMUM EFFICIENCY POINT FOR AMBIENT AND CRYOGENIC OPERATIONS (% VARIATIONS W.R.T. AMBIENT CONDITIONS)

	Ambient temperature	Cryogenic temperature	
Maximum efficiency, (%)	63.0 (s=10.9%)	85.2 (s=4.0%)	+35%
Stator current, (A)	3.3	6.7	+103%
Torque, (Nm)	0.72	1.95	+171%
Rotor speed, (rpm)	1353	1441	+7%
Mechanical output Power, (W)	102.0	294.3	+189%
Mechanical losses, (W)	1.96	3.83	+95%
Iron losses, (W)	12.5	14.5	+16%
Stator Joule losses, (W)	35.9	23.3	-35%
Rotor Joule losses, (W)	9.6	9.5	-1%

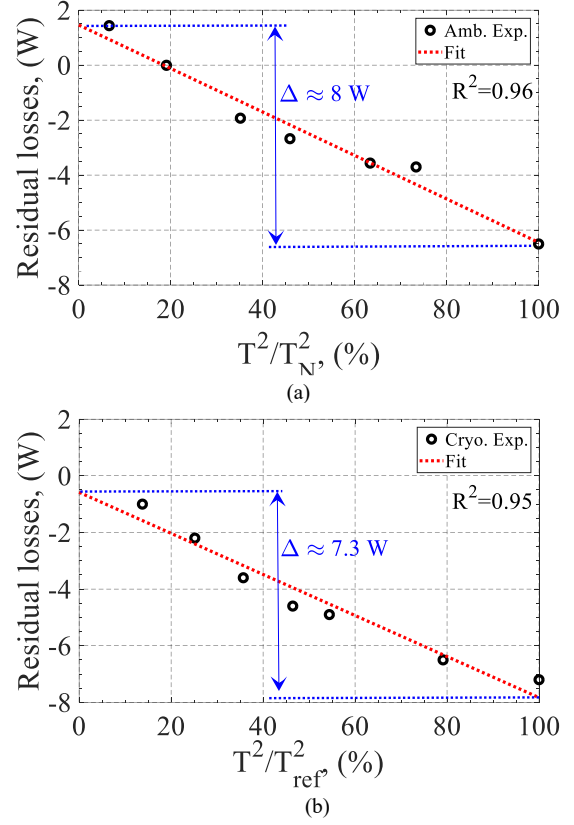


Fig. 8: Residual losses for the 90 W IM at (a) ambient temperature and (b) cryogenic conditions.

The mechanical,  $P_{mec}$ , and iron losses,  $P_{fe}$ , are determined from the no-load tests. Rotor losses,  $P_r$ , are obtained using (1) where  $s$  is the slip.

$$P_r = (P_{in} - P_{cus} - P_{fe})s \quad (1)$$

In Fig. 7, the measured input power,  $P_{in}$ , is marked in a red line. At rated voltage and frequency, according to the input-output method, the machine presents a maximum efficiency of 63.0% (with a torque of 0.72 Nm) at ambient conditions and 85.2% (with a torque of 1.95 Nm) at cryogenic conditions. This is mainly due to the high decrease of stator windings and rotor losses and the exceptional cooling capacity of the liquid nitrogen. These torques have been assumed as the reference torques to carry out the variable load tests used for the residual losses computation.

Moreover, Fig. 7b shows the separation of active power for the two testing conditions, side by side, to facilitate the comparison between ambient temperature and cryogenic results. Under cryogenic conditions, the reference torque,  $T_{ref}$ , corresponds to the maximum efficiency point. As it can be seen, it is possible to achieve a higher maximum torque from 0.72 Nm at ambient conditions to 3.4 Nm at cryogenic conditions. The maximum torque of 3.4 Nm, at cryogenic conditions, was obtained with an efficiency of 73%. This efficiency is still higher than the maximum efficiency obtained from ambient conditions. Table IV presents the 90 W IM performance at the maximum efficiency point for ambient and cryogenic conditions.

TABLE V STEADY-STATE EQUIVALENT CIRCUIT PARAMETERS AT 50 HZ FOR THE 550 W IM AT AMBIENT AND CRYOGENIC CONDITIONS

Parameter	Amb.	Cryo.	Difference
$R_s$	18.1 $\Omega$	2.90 $\Omega$	-84.0%
$R'_r$	14.6 $\Omega$	5.8 $\Omega$	-60.3%
$X_{\sigma s}$	17.0 $\Omega$	15.7 $\Omega$	-7.6%
$X'_{\sigma r}$	17.0 $\Omega$	15.7 $\Omega$	-7.6%
$R_{fe}$	4924.5 $\Omega$	4403.4 $\Omega$	-10.6%
$X_m$	169.8 $\Omega$	165.4 $\Omega$	-2.6%

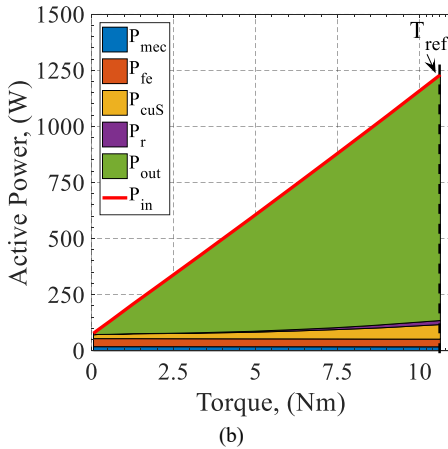
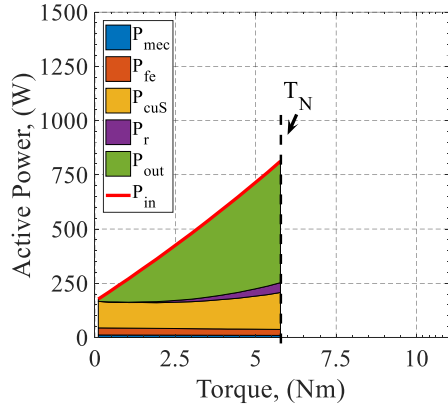


Fig. 9. Separation of active power into losses and output power for the 550 W IM at (a) ambient temperature, and (b) cryogenic conditions.

In Fig. 8, the residual losses are shown as a function of the torque square normalized to its rated value, for ambient conditions, and to its reference torque (maximum efficiency point) for cryogenic conditions. These have similar behaviors and account for 4.1% and 2.1% of the input power for the maximum efficiency point, under ambient and cryogenic conditions, respectively. Despite having a negative slope, the correlation factors satisfy the minimum standard requirements, being 0.96 and 0.95, respectively. There is a slight decrease in the variation of the residual losses,  $\Delta$ , between no-load and rated load from ambient to cryogenic conditions. To better understand the behavior of residual losses, the same experimental results were carried out in a 550 W induction machine.

TABLE VI SUMMARIZED PERFORMANCE FOR THE 550 W IM AT MAXIMUM EFFICIENCY POINT FOR AMBIENT AND CRYOGENIC OPERATIONS (% VARIATIONS W.R.T. AMBIENT CONDITIONS)

	Ambient temperature	Cryogenic temperature	
Maximum efficiency, (%)	68.3 (s=7.3%)	88.9 (s=1.6%)	+30%
Stator current, (A)	1.78	2.73	+53%
Torque, (Nm)	5.77	10.6	+84%
Rotor speed, (rpm)	927	984	+6%
Mechanical output Power, (W)	560	1096	+96%
Mechanical losses, (W)	4.5	11.1	+146%
Iron losses, (W)	26.7	34.3	+28%
Stator Joule losses, (W)	171.2	64.9	-62%
Rotor Joule losses, (W)	45.4	18.0	-60%

### B. 550 W Induction Motor

The same experimental no-load, locked rotor and load tests were performed on the 550 W, 400 V, 6 pole IM. Table V reports the IM steady-state equivalent circuit parameters calculated from the no-load and locked rotor tests at ambient and cryogenic conditions. As expected, due to the decrease of temperature, the stator windings resistance decreases of approximately 84%, which is in line with the drop of resistivity of copper under cryogenic conditions reported in [5], and the results found for the tested 90 W IM. The rotor resistance decreases approximately of 60.3%, which is lower than the resistance drop found for the 90 W IM. This effect can be related to different rotor aluminum materials used on the 550 W IM and the different impact of the skin effect. In fact, different aluminum alloys present different resistivities under cryogenic conditions, and a larger size of the rotor cage cross-section also results in a higher skin effect [5].

Different than in the 90 W IM, a small change in the stator and rotor reactances has been found for the 550 W motor. This is in line with a higher impact of the skin effect. A drop of 10.6% of the iron losses resistance was verified, corresponding to an increase of 11.2% of iron losses at rated voltage, which is coherent with the findings for the 90 W IM and in [7] and [11]. Also, it was observed an increase of 115% of mechanical losses,  $P_{mec}$ , from 5.4 W under ambient conditions to 11.6 W under cryogenic conditions. This increase is slightly higher but also in line with the one observed for the 90 W IM (+95.4%). In the authors' opinion, this effect could be explained by the increase in size and weight of the 550 W IM.

The results from the load tests conducted on the 550 W motor are presented in Fig. 9 for ambient and cryogenic conditions. At ambient temperature conditions, the rated torque, speed, efficiency, and output power are 5.77 Nm, 927 rpm, 68.3% and 560 W, respectively.

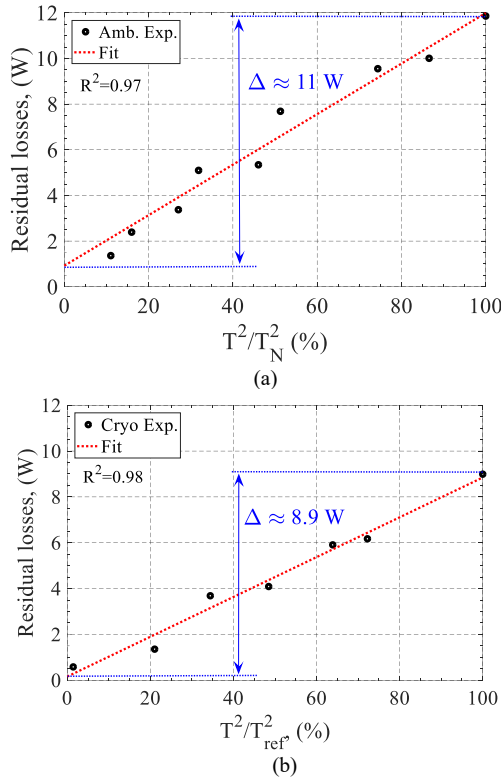


Fig. 10. Residual losses for the 550 W IM at (a) ambient temperature and (b) cryogenic conditions.

At cryogenic conditions and the maximum efficiency point, the reference torque, speed, efficiency, and output power are 10.6 Nm, 984.1 rpm, 88.9% and 1095.8 W, respectively. From Fig. 9, it can also be seen that the stator copper and rotor losses highly decrease under cryogenic conditions, as expected.

In Table VI is shown a comparison of the 550 W IM performance between ambient and cryogenic conditions, for the maximum efficiency point. Under cryogenic conditions, there is an increase of 30% of efficiency and a 96% increase of output power. Please note that under cryogenic conditions, despite the decrease of 10.6% of iron losses resistance, the iron losses increase by 28% due to higher magnetizing voltage resultant from the lower stator voltage drop.

The residual losses for the 550 W IM at ambient and cryogenic conditions are shown in Fig. 10 as a function of the torque square normalized to its rated value,  $T_N$ , under ambient temperature, and to its reference value,  $T_{ref}$ , under cryogenic conditions. Both have similar behaviors and account for 1.3% and 0.7% of the input power for the best efficiency point, under ambient and cryogenic conditions, respectively. The variation of the residual losses,  $\Delta$ , between no-load and rated load, reduces from 11 W, under ambient conditions, down to 8.9 W, under cryogenic conditions.

#### IV. DISCUSSION

When submerged in liquid nitrogen, both 90 W and 550 W induction machines present an enhancement of performance, however with different relative values. In Table VII are presented the change of their equivalent circuit parameters when submitted to cryogenic conditions.

TABLE VII COMPARISON OF THE EQUIVALENT CIRCUIT PARAMETERS AT CRYOGENIC CONDITIONS

Parameter	90 W IM	550 W IM
$R_S$	-84.1%	-84.0%
$R'_r$	-73.4%	-60.3%
$X_{\sigma s}$	0%	-7.6%
$X'_{\sigma r}$	0%	-7.6%
$R_{fe}$	-10.4%	-10.6%
$X_m$	-1.2%	-2.6%

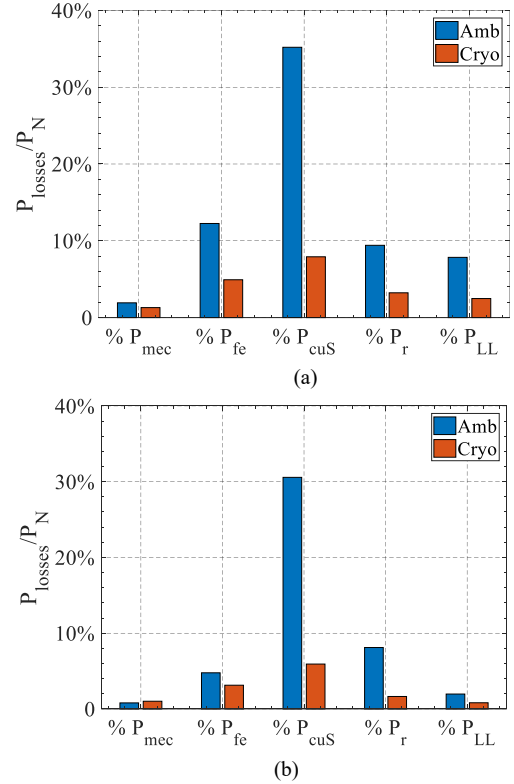


Fig. 11. Ratio between losses and rated power for ambient and cryogenic conditions: (a) 90 W IM, and (b) 550 W IM.

The stator resistance  $R_S$ , iron losses resistance  $R_{fe}$ , and magnetizing reactance  $X_m$ , present a similar relative reduction. However, the rotor resistance,  $R'_r$ , presents a lower reduction for the 550 W IM, mainly due to the different aluminum alloy used in the rotor cage and due to the higher impact of the skin effect under cryogenic conditions. The presence of the skin effect is also visible in the change of -7.6% on the stator and rotor reactances,  $X_{\sigma s}$  and  $X'_{\sigma r}$ , for the 550 W. Further research is being developed using different power machines with the same materials to separate the influence of the skin effect for higher power induction machines.

The output power and efficiency increase are higher for the 90 W IM. For this IM, the output power and efficiency increased +189% and +35%, respectively, and increased +96% and +30% for the 550 W IM, respectively. This is mainly due to the higher weight of stator copper losses on the 90 W IM than on the 550 W IM at ambient temperature conditions.

The reduction of the stator resistance,  $R_s$ , obtained under cryogenic conditions, allows a higher increase of +103% of stator current for the 90 W IM compared with the increase of +53% for the 550 W IM. This leads to a higher increase of output torque for the 90 W IM.

Another interesting effect is the weight of the iron losses on the efficiency. At ambient temperature conditions, these contribute to around 7.7% and 3.3% of the input power, for the 90 W and 550 W IMs, respectively. These contributions reduce to around 4.2% for the cryogenic 90 W IM, and to 2.8% for the cryogenic 550 W IM. This means that despite the typical increase of iron losses under cryogenic operation, the weight of these losses decreased for a higher power IM, thus mitigating their effect on the machine performance.

A comparison of the losses normalized to the rated power for the 90 W and 550 W IMs is presented in Fig. 11 at ambient and cryogenic conditions. The stator copper and rotor losses have the highest reduction. Iron and residual losses are also reduced, while the mechanical losses for the 550 W present a slight increase. Please note that this is an initial comparison between two different machines; therefore, a more extensive study must be carried out. To avoid the influence of different materials in this analysis, different ranges of IMs must be tested using the same materials, and preferable from the same manufacturer to account for the same manufacturing and design techniques.

## V. CONCLUSION

This work presents a loss analysis of induction motors operated under cryogenic conditions by immersion in liquid nitrogen. Two induction machines respectively rated 90 W and 550 W were experimentally tested. No-load, locked rotor and load tests were performed on both IMs, at ambient and cryogenic conditions. The no-load and locked rotor tests were carried out to determine the IMs equivalent circuit parameters and the mechanical and iron losses. Load tests were done to evaluate the machine performance and the separation of active power into output power and losses and to evaluate the evolution of residual losses. In addition, for the 90 W IM the evolutions of the mechanical losses and the iron losses resistance were evaluated for different electric frequencies and compared between ambient temperature and cryogenic conditions.

Under cryogenic conditions, results show a substantial decrease of stator resistances, around -84%, and rotor resistances, between -60% to -73%. The mechanical losses presented an increase of around 100%, and the iron losses increased, leading to a decrease of iron losses resistance between 5% and 10%. Due to the decrease of stator copper and rotor resistances, and the high cooling capabilities of liquid nitrogen, both IMs experienced an increase of output power, between +96% and +189%, and an increase of efficiencies, between 30% and 35%, under cryogenic conditions. Regarding the residual losses, both IMs present a linear behavior with the torque squared at ambient temperature and cryogenic conditions. The variation of the residual losses between no-load and rated load presented a decrease under cryogenic conditions.

Further research will concentrate on different ranges of IMs using similar materials and constructed with similar design and manufacturing techniques.

## ACKNOWLEDGMENT

This work was partially financed by national funds through FCT – Foundation for Science and Technology, I.P., through IDMEC, under LAETA, project UIDB/50022/2020.

## REFERENCES

- [1] United Nations General Assembly. “Transforming Our World: The 2030 Agenda for Sustainable Development”. A/RES/70/1, 2015.
- [2] European Commission. “Flightpath 2050: Europe’s Vision for Aviation—Report of the High-Level Group on Aviation Research”, 2011.
- [3] H. M. Kim, K. W. Lee, D. G. Kim, J. H. Park, and G. S. Park, “Design of Cryogenic Induction Motor Submerged in Liquefied Natural Gas,” in *IEEE Trans. Magn.*, vol. 54, no. 3, pp. 1–4, March 2018.
- [4] J. H. Redmond, and F. W. Bott. “Development of Cryogenic Electric Motors,” *SAE Transactions*, vol. 72, 1964.
- [5] A. F. Clark, G.E. Childs, G.H. Wallace, “Electrical resistivity of some engineering alloys at low temperatures”, *Cryogenics*, vol. 10, no. 4, pp. 295-305, 1970.
- [6] F. R. Flickett, “Electrical properties of materials and their measurement at low temperatures”, U.S. Dep. of Commerce, NBS Technical note, 1982.
- [7] X. Lv, D. Sun and L. Sun, “Determination of Iron Loss Coefficients of Ferromagnetic Materials Used in Cryogenic Motors,” 2019 22nd International Conference on Electrical Machines and Systems (ICEMS), pp. 1-5, 2019.
- [8] X. Pei, A. C. Smith, L. Vandenbossche and J. Rens, “Magnetic Characterization of Soft Magnetic Cores at Cryogenic Temperatures,” in *IEEE Trans. Appl. Supercond.*, vol. 29, no. 5, pp. 1-6, Aug. 2019.
- [9] D. Miyagi, D. Otome, M. Nakano and N. Takahashi, “Measurement of Magnetic Properties of Nonoriented Electrical Steel Sheet at Liquid Nitrogen Temperature Using Single Sheet Tester,” in *IEEE Trans. Magn.*, vol. 46, no. 2, pp. 314-317, Feb. 2010.
- [10] A. Chengliu, H. Yuanfeng and W. Haifeng, “Main losses study of cryogenic induction motor for submerged liquid natural gas pump,” 2015 18th International Conference on Electrical Machines and Systems (ICEMS), pp. 133-136, 2015.
- [11] M. Biasion, J.F.P. Fernandes, P. J. Costa Branco, S. Vaschetto, A. Cavagnino and A. Tenconi, “A Comparison of Cryogenic-Cooled and Superconducting Electrical Machines”, 2021 IEEE Energy Conversion Congress and Exposition (ECCE), 2021, pp 4045-4052.
- [12] A. G. Pronto, M. V. Neves, and A. L. Rodrigues, “A possible solution to reduce magnetic losses in transformer cores working at liquid nitrogen temperature,” *Physica Procedia*, vol. 36, pp. 1103-1108, 2012.
- [13] M. Miyamoto, T. Matsuo, and T. Nakamura, “Measurement of vector hysteretic property of silicon steel sheets at liquid nitrogen temperature”. *Przeegląd Elektrotechniczny*, vol. 87, no. 9b, p. 4, 2011.
- [14] D. Miyagi, K. Miki, M. Nakano and N. Takahashi, “Influence of Compressive Stress on Magnetic Properties of Laminated Electrical Steel Sheets,” in *IEEE Trans. Magn.*, vol. 46, no. 2, pp. 318-321, Feb. 2010.
- [15] K. Tsugunori, Y. Kido, A. Kutsukake, T. Ikeda, and M. Enokizono, “Magnetic properties of soft magnetic materials under tensile and compressive stress.” *Przeegląd Elektrotechniczny*, vol. 87, no. 9b, 2011.
- [16] Vrancik, J. E.. “Prediction of windage power loss in alternators.”, Nasa Technical Note, TN D-4849, 1968.
- [17] A. B. Nachouane, A. Abdelli, G. Friedrich and S. Vivier, “Estimation of windage losses inside very narrow air gaps of high speed electrical machines without an internal ventilation using CFD methods,” 2016 XXII International Conference on Electrical Machines (ICEM), 2016, pp. 2704-2710.
- [18] P. M. Wild, N. Djilali, and G. W. Vickers, “Experimental and computational assessment of windage losses in rotating machinery,” *Journal of Fluids Engineering*, vol. 118, no.1, pp. 116-122, 1996.
- [19] L. F. D. Bucho, J. F. P. Fernandes, M. Biasion, S. Vaschetto and A. Cavagnino, “Experimental Assessment of Cryogenic Cooling Impact on Induction Motors,” in *IEEE Trans. Energy Convers.*, 2022.
- [20] M. Biasion, I. Peixoto, J. F. P. Fernandes, S. Vaschetto, G. Bramerdorfer, A. Cavagnino, “Iron Loss Characterization in Laminated Cores at Room and Liquid Nitrogen Temperature”, 2022 IEEE Energy Conversion Congress and Exposition (ECCE), 2022.